J|A|C|S ARTICLES

Published on Web 03/30/2009

# Conformation of Receptor Adopted upon Interaction with Virus Revealed by Site-Specific Fluorescence Quenchers and FRET Analysis

Jürgen Wruss,[†] Philipp D. Pollheimer,[‡] Irene Meindl,[‡] Annett Reichel,[§] Katrin Schulze,[§] Wolfgang Schöfberger,[‡] Jacob Piehler,[§] Robert Tampé,[§] Dieter Blaas,[†] and Hermann J. Gruber*[,‡]

*Max F. Perutz Laboratories, Institute of Medicinal Biochemistry, Dr. Bohr Gasse 9/3, Medical University of Vienna, Vienna A-1030, Austria, Institute of Biophysics and Institute of Inorganic Chemistry, University of Linz, Altenberger Strasse 69, A-4040 Linz, Austria, and Institute of Biochemistry, Biocenter, Johann Wolfgang Goethe-University, Max-von-Laue-Strasse 9, D-60438 Frankfurt a. M., Germany*

Received October 7, 2008; E-mail: hermann.gruber@jku.at

***Abstract:*** Human rhinovirus serotype 2 (HRV2) specifically binds to very-low-density lipoprotein receptor (VLDLR). Among the eight extracellular repeats of VLDLR, the third module (V3) has the highest affinity for the virus, and 12 copies of the genetically engineered concatamer V33333-$His_6$ were found to bind per virus particle. In the present study, ring formation of V33333-$His_6$ about each of the 12 5-fold symmetry axes on HRV2 was demonstrated by fluorescence resonance energy transfer (FRET) between donor and acceptor on N- and C-terminus, respectively. In particular, the N-terminus of V33333-$His_6$ was labeled with fluorescein, and the C-terminus with a new quencher which was bound to the $His_6$ tag with nanomolar affinity ($K_d \sim 10^{-8}$ M) in the presence of 2 $\mu$M $NiCl_2$.

## Introduction

Human rhinoviruses (HRVs), the main cause of common colds, use two different types of receptors for infection; major group HRVs (87 types) bind intercellular adhesion molecule 1, whereas minor group viruses (12 types, including HRV2)[1] gain access to the host cell via members of the low-density lipoprotein receptor (LDLR) family, including LDLR proper and LDLR-related protein (LRP).[2] Although very-LDLR (VLDLR) is probably not involved in infection of the nasal epithelia, minor group HRVs bind this receptor even more strongly.[3−6] Several of the modules making up the N-terminal ligand-binding domains of these proteins contribute to binding of various cognate ligands, such as lipoproteins, proteases/inhibitors, signaling factors, toxins, and many others, including HRVs.[7] For the latter, numerous studies have been carried out with genetically engineered derivates of human VLDLR; as the ligand-binding modules (eight in case of VLDLR) are not identical in sequence, interpretation of the binding data was facilitated by the use of concatemers of repeat number 3 (V3). For ease of expression and purification, oligomers of V3 fused N-terminally to maltose binding protein (MBP) and C-terminally to a $His_6$ tag were employed in affinity measurements,[6,8] determination of the stoichiometry,[3] and atomic force microscopy.[9,10] The binding avidity strongly increased with the number of copies of V3 in the construct; up to 12 molecules of MBP-V33333-$His_6$ were found to bind per virus particle, and X-ray crystallography of complexes between V23-$His_6$ and HRV2 revealed a close vicinity of N- and C-terminus of two adjacent modules bound to the virion.[11] These data strongly suggested that individual V33333-$His_6$ molecules wrap around each 5-fold axis of icosahedral symmetry. Consequently, the N- and C-terminus of the same molecule should come close to each other. In order to prove this hypothesis, we decided to attach a single fluorescein residue to the N-terminus and a single quencher dye to the C-terminus of V33333-$His_6$ and to measure fluorescence resonance energy transfer (FRET) in the absence and presence of virus particles, as depicted in Scheme 1.

For selective labeling of the C-terminus with an acceptor dye, the most straightforward method appeared to be $Ni^{2+}$-mediated

[†] Medical University of Vienna.
[‡] University of Linz.
[§] Johann Wolfgang Goethe-University.

(1) Vlasak, M.; Roivainen, M.; Reithmayer, M.; Goesler, I.; Laine, P.; Snyers, L.; Hovi, T.; Blaas, D. *J. Virol.* **2005**, *79*, 7389–7395.
(2) Hofer, F.; Gruenberger, M.; Kowalski, H.; Machat, H.; Huettinger, M.; Kuechler, E; Blaas, D. *Proc. Natl. Acad. Sci. U.S.A.* **1994**, *91*, 1839–1842.
(3) Konecsni, T.; Kremser, L.; Snyers, L.; Rankl, C.; Kilar, F.; Kenndler, E.; Blaas, D. *FEBS Lett.* **2004**, *568*, 99–104.
(4) Marlovits, T. C.; Abrahamsberg, C.; Blaas, D. *J. Virol.* **1998**, *72*, 10246–10250.
(5) Ronacher, B.; Marlovits, T. C.; Moser, R.; Blaas, D. *Virology* **2000**, *278*, 541–550.
(6) Wruss, J.; Rünzler, D.; Steiger, C.; Chiba, P.; Köhler, G.; Blaas, D. *Biochemistry* **2007**, *46*, 6331–6339.
(7) Nykjaer, A.; Willnow, T. E. *Trends Cell Biol.* **2002**, *12*, 273–280.
(8) Moser, R.; Snyers, L.; Wruss, J.; Angulo, J.; Peters, H.; Peters, T.; Blaas, D. *Virology* **2005**, *338*, 259–269.
(9) Kienberger, F.; Rankl, C.; Pastushenko, V.; Zhu, R.; Blaas, D.; Hinterdorfer, P. *Structure (Camb.)* **2005**, *13*, 1247–1253.
(10) Rankl, C.; Kienberger, F.; Wildling, L.; Wruss, J.; Gruber, H. J.; Blaas, D.; Hinterdorfer, P. *Proc. Natl. Acad. Sci. U.S.A.* **2008**, *105*, 17778–17783.
(11) Verdaguer, N.; Fita, I.; Reithmayer, M.; Moser, R.; Blaas, D. *Nature Struct. Mol. Biol.* **2004**, *11*, 429–434.

 **10.1021/ja807917t CCC: $40.75** 

***Scheme 1.*** The VLDL-Receptor Derivate V33333-$His_6$ Lacking Lysine Residues Was Labeled at Its N-Terminus with 6-Carboxyfluorescein (A) and QSY7−S-Tris-NTA (**3**, Chart 1) Was Bound to the C-Terminal $His_6$ Tag (B)[a]

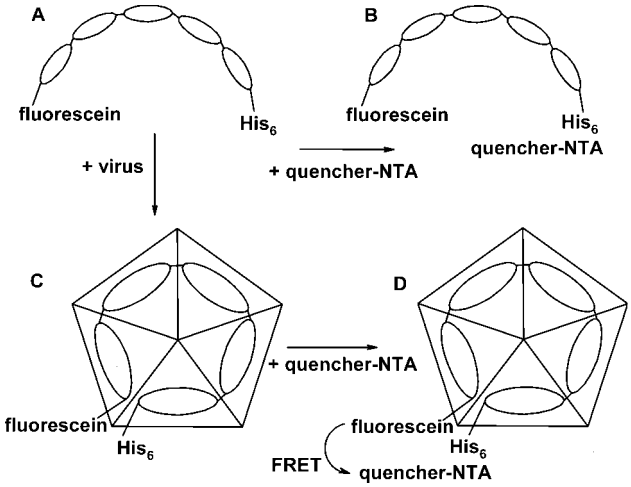


[a] Alternatively, fluorescein-labeled V33333-$His_6$ was first bound to virus particles (C) and QSY7−S-tris-NTA was added (D). The corresponding fluorescence data are reported in Table 1. Note that the scheme in C and D is not drawn to scale; the receptor attaches much closer to the vertex (i.e., the axis of 5-fold icosahedral symmetry). The virus capsid is built from 12 such pentamers.

***Chart 1.*** Structures of Flu-$His_6$ (**1**), QSY7−NTA (**2**), and QSY7−S-Tris-NTA (**3**)

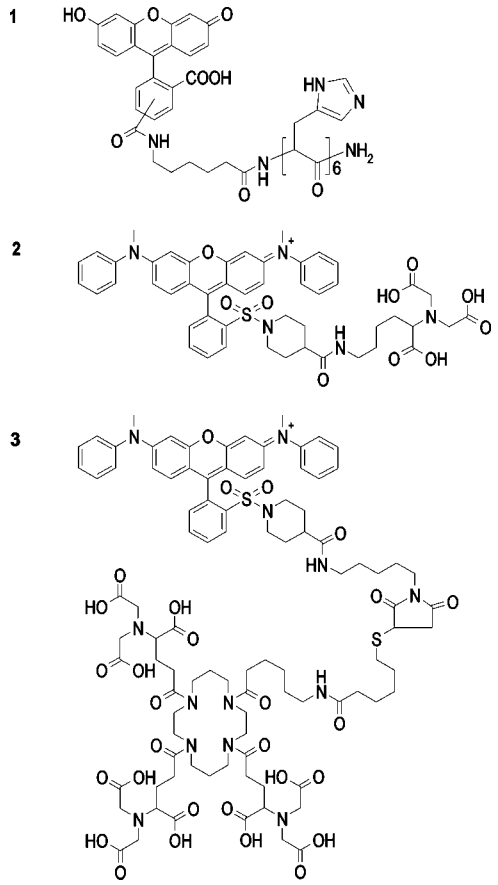


coordinative binding of a quencher−NTA conjugate (Scheme 1) of which several kinds were known before this study.[12−15] The following properties are desirable for a quencher−NTA conjugate to be used in FRET studies: (i) high affinity for $His_6$ tags, (ii) high quenching efficiency of a suitable donor fluorophore, (iii) minimal emission by the quencher, and (iv) ease of chemical synthesis, since no quencher−NTA conjugate is commercially available so far. Quenchers with three simultaneously attached NTA groups ("tris-NTA") show unparalleled affinity for $His_6$ tags ($K_d \sim 10^{-8}$ M),[13−16] but evidence for high quenching efficiency was missing until very recently.[16] We therefore tested QSY7−NTA (Chart 1), the conjugate of NTA with the nonemitting dye QSY7 that had been designed for maximal quenching of fluorescein or green fluorescent protein (>90%).[12] Unfortunately, the single NTA function of QSY7−NTA did not provide for sufficient affinity for $His_6$-tagged proteins under physiological conditions; thus, a new tris-NTA derivative of QSY7 was synthesized which proved ideal for demonstration of intramolecular FRET according to Scheme 1.

***Table 1.*** Quenching of Fluorescein-Labeled $His_6$-Tagged Proteins in the Absence and Presence of Virus[a]

| | control | $Ni^{2+}$-indep effect | $Ni^{2+}$-dep effect | effect of virus |
|---|---|---|---|---|
| | Reagents (nM) | | | |
| HRV2 | − | − | − | 1.7[b] |
| EDTA | 10 | 10 | − | − |
| QSY7−S-tris-NTA | − | 100 | 100 | 100 |
| | Fluorescence (%) | | | |
| Flu-MBP[c] | 100 ± 1 | 98 ± 2 | 99 ± 2 | 96 ± 8 |
| Flu-MBP-$His_6$[d] | 100 ± 1 | 93 ± 1 | 21 ± 1 | 13 ± 1 |
| Flu-MBP-V333-$His_6$[e] | 100 ± 2 | 101 ± 3 | 51 ± 1 | 51 ± 3 |
| Flu-MBP-V33333-$His_6$[e] | 100 ± 2 | 96 ± 1 | 64 ± 5 | 32 ± 2 |
| Flu-V33333-$His_6$[f] | 100 ± 3 | 99 ± 3 | 99 ± 3 | 18 ± 4 |

[a] Binding of QSY7−S-tris-NTA to fluorescein-labeled proteins (10 nM) was measured in the absence or presence of EDTA, QSY7−S-tris-NTA, and virus. Fluorescence intensity is related to the unquenched control (set to 100% by definition). All experiments were performed in HBS−Ca-Ni (150 mM NaCl, 20 mM HEPES, 2 mM $CaCl_2$, adjusted to pH = 7.4 with NaOH and subsequently to 2 $\mu$M $NiCl_2$ with 10 mM $NiCl_2$). Each experiment was carried out in triplicate to determine standard deviations of the mean. [b] Corresponding to 12 × 1.7 nM = 20.4 nM binding sites for V33333-$His_6$. [c] 1.8 labels/protein. [d] 3.6 labels/protein. [e] 0.9 labels/protein. [f] 0.7 labels/protein.

## Materials and Methods

**Materials.** Fluorescein-labeled hexahistidine (Flu-$His_6$, **1**, Chart 1), QSY7-labeled derivatives of mono-NTA (QSY7−NTA, **2**, Chart 1), and tris-NTA (QSY7−S-tris-NTA, **3**, Chart 1), as well as virus particles and labeled proteins, were prepared as described in the Supporting Information.

**Protocol for the Quenching Experiments Reported in Table 1.** All experiments were performed in HBS−Ca-Ni (150 mM NaCl, 20 mM HEPES, 2 mM $CaCl_2$ [for maintaining the native conformation of V33333],[17] 2 $\mu$M $Ni^{2+}$ [for tight binding of QSY7−S-tris-NTA to $His_6$, see Figure S8 in the Supporting Information], pH = 7.4) in a final volume of 500 $\mu$L. HBS-Ca could be stored frozen, but HBS−Ca-Ni could not, because the minute amount of nickel ions used was obviously lost by precipitation or adsorption to the wall of the bottle.

(12) Guignet, E. G.; Hovius, R.; Vogel, H. *Nat. Biotechnol.* **2004**, *22*, 440–444.
(13) Huang, Z.; Park, J. I.; Watson, D. S.; Hwang, P.; Szoka, F. C., Jr. *Bioconjugate Chem.* **2006**, *17*, 1592–1600.
(14) Lata, S.; Reichel, A.; Brock, R.; Tampé, R.; Piehler, J. *J. Am. Chem. Soc.* **2005**, *127*, 10205–10215.
(15) Lata, S.; Gavutis, M.; Tampé, R.; Piehler, J. *J. Am. Chem. Soc.* **2006**, *128*, 2365–2372.
(16) Strunk, J. J.; Gregor, I.; Becker, Y.; Lamken, P.; Lata, S.; Reichel, A.; Enderlein, J.; Piehler, J. *Bioconjugate Chem.* **2009**, *20*, 41–46.
(17) Atkins, A. R.; Brereton, I. M.; Kroon, P. A.; Lee, H. T.; Smith, R. *Biochemistry* **1998**, *37*, 1662–1670.

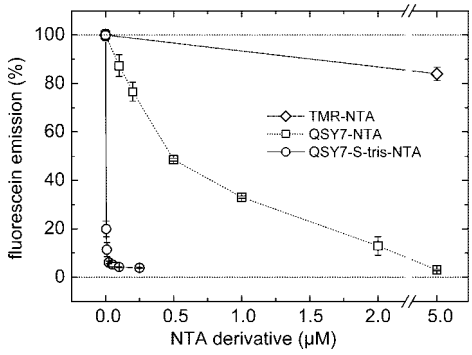


***Figure 1.*** Titration of Flu-$His_6$ (25 nM) with TMR-NTA-Ni (diamonds) and QSY7−NTA-Ni (squares) in buffer A (300 mM NaCl, 50 mM $NaH_2PO4$, 80 $\mu$M $C_{12}E_8$, adjusted to pH = 8.0 with NaOH) while measuring fluorescein emission at 525 nm (excitation at 485 nm) after 30 min incubation time. Alternatively, Flu-$His_6$ (10 nM) was titrated with QSY7−S-tris-NTA (circles) in buffer B (150 mM NaCl, 20 mM boric acid, adjusted to pH = 7.4 with NaOH) containing 2 $\mu$M $NiCl_2$ in all samples except for the first one which contained neither NTA derivative nor $NiCl_2$ but 1 mM EDTA (fluorescence emission set to 100% = absence of quenching).

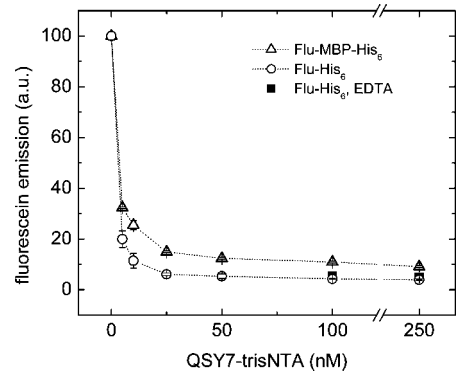


***Figure 2.*** Titration of Flu-$His_6$ (circles, 10 nM in 150 mM NaCl, 20 mM boric acid, pH 7.4 adjusted with NaOH; buffer B) and of Flu-MBP-$His_6$ (triangles, 5.8 nM protein with 1.8 labels per protein, in HBS−Ca-Ni) with QSY7−S-tris-NTA while measuring fluorescein emission at 525 nm (excitation at 485 nm) after 30 min incubation time. All samples contained 2 $\mu$M $NiCl_2$. Data obtained in the presence of EDTA (5 mM) instead of QSY7−S-tris-NTA were set to 100% fluorescence emission (absence of quenching). After measurement of fluorescence, the Flu-$His_6$ samples with 100 and 250 nM QSY7−S-tris-NTA were adjusted to 5 mM EDTA, incubated for 1 h, and remeasured (solid squares).

For "unquenched controls" (first data column), fluorescein-labeled protein (50 $\mu$L, 100 nM label concentration, in HBS-Ca) was mixed with EDTA (50 $\mu$L, 100 mM stock solution in water, pH adjusted to 7.4 with NaOH), diluted to 500 $\mu$L with HBS−Ca-Ni, and incubated for 30 min at room temperature, and fluorescein emission was measured at 525 nm (excitation at 485 nm). The high final EDTA concentration (10 mM) was chosen to perfectly mask all transition metal ions despite the relatively high $Ca^{2+}$ concentration (2 mM). For the "nickel-independent effect" (second data column), mixing of labeled protein (50 $\mu$L, 100 nM label concentration) with EDTA (50 $\mu$L, 100 mM) was followed by addition of HBS−Ca-Ni (300 $\mu$L) and QSY7−S-tris-NTA (100 $\mu$L, 500 nM, in HBS−Ca-Ni) and fluorescence was read after 30 min. For measurement of the "nickel-dependent effect" (third data column), labeled protein (50 $\mu$L, 100 nM label concentration) was diluted to 400 $\mu$L with HBS−Ca-Ni and mixed with QSY7−S-tris-NTA (100 $\mu$L 500 nM, in HBS−Ca-Ni). For the last data column, fluorescein-labeled protein (50 $\mu$L, 100 nM in HBS-Ca) was mixed with HRV2 (3.4 $\mu$L, 2 mg/mL = 250 nM virus = 3 $\mu$M receptor binding sites, in HBS) and incubated for 15 min, followed by addition of HBS−Ca-Ni (345 $\mu$L) and QSY7−S-tris-NTA (100 $\mu$L, 500 nM) and another 15 min incubation period.

## Results

In the present study, the hypothesis of ring formation by virus-bound V33333-$His_6$ was tested by FRET from a donor fluorophore at the N-terminus to an acceptor dye at the C-terminus (see Scheme 1). Specific attachment of a single fluorescein residue to the N-terminus was easy (see Supporting Information) because V33333 lacks lysines.[8] For selective labeling of the C-terminus with an acceptor dye, the most straightforward method appeared to be $Ni^{2+}$-mediated binding of a quencher−NTA conjugate (Scheme 1).

In exploratory test series, fluorescein-labeled $His_6$ peptide (**1**, Flu-$His_6$, see Chart 1) was used as a substitute for a fluorescein-labeled $His_6$-tagged protein, thereby simplifying data interpretation. QSY7−NTA (**2**, see Chart 1) was chosen as the first quencher−NTA candidate because it can be prepared from commercial reagents in one step[12] and because QSY7 is a nonfluorescent analogue of tetramethylrhodamine (TMR) with superior quenching properties. As expected, Flu-$His_6$ was much more efficiently quenched by QSY7−NTA-Ni (Figure 1, squares) than by TMR-NTA-Ni (diamonds). Nevertheless, QSY7−NTA was abandoned for the following reasons: (i) In our hands, the published synthesis gave a yield of only 4−5% with respect to the expensive dye precursor. (ii) Consumption was high because full quenching required 5 $\mu$M QSY7−NTA. (iii) Finally, strong quenching was only seen in the published buffer (containing 80 $\mu$M of the detergent $C_{12}E_9$, pH 8.0)[12] but not under more physiological conditions (data not shown).

These problems were solved by replacing the mono-NTA function in QSY7−NTA with tris-NTA which is known to bind $His_6$ tags with much higher affinity ($K_d$ = 5−25 nM).[13−16] Thiol-maleimide coupling was chosen for the synthesis of QSY7−S-tris-NTA (**3**, see Chart 1), and the yield was 89% with respect to QSY7−maleimide. QSY7−S-tris-NTA met the highest expectations in terms of quenching efficiency and affinity for Flu-$His_6$ (circles in Figure 1), as long as $NiCl_2$ was included at 1−2 $\mu$M concentration (see Figure S8 in the Supporting Information). In Figure 2, the same data with QSY7−S-tris-NTA and Flu-$His_6$ are shown on an expanded concentration scale (circles). Here it can be seen that quenching reached a plateau around 25 nM (94.1 ± 0.5%) that slightly increased to 95.7 ± 0.3% at 100 nM. The latter condition was chosen to study the virus−receptor interaction (Table 1). The strong quenching seen even at 10 nM QSY7−S-tris-NTA indicates an effective $K_d$ of <10 nM.

Essentially the same affinity and very similar FRET efficiency were also observed with Flu-MBP-$His_6$ (Figure 2, triangles). The degree of fluorescence quenching at 100 nM QSY7−S-tris-NTA was slightly lower for Flu-MBP-$His_6$ than for Flu-$His_6$ (89.1 ± 0.4% versus 95.7 ± 0.3%), but this was expected in view of the much larger size of the protein ($M_r$ = 43,619 versus 1236) which leads to longer average distances between donor and acceptor dye. The interaction of QSY7−S-tris-NTA with the protein was strictly dependent on the $His_6$-tag, since only Flu-MBP-$His_6$ was quenched by QSY7−S-tris-NTA in the presence of $NiCl_2$, while Flu-MBP was not (see Table 1). Once formed, the complex between QSY7−S-tris-NTA-$Ni^{2+}$ and Flu-$His_6$ was fully resistant to addition of EDTA (5 mM) on the time scale of 1 h. This was deduced from equally strong quenching prior to addition of EDTA (Figure 2, open circles) and after incubation in 5 mM EDTA (Figure 2, solid squares).

After the above model experiments, the assay system was ready to be applied to the virus−receptor problem. This was done in two ways, either with one fluorescein label at the N-terminus (Flu-V33333-$His_6$), as depicted in Scheme 1, or with fluorescein-labeled MBP at the N-terminus (Flu-MBP-V33333-$His_6$). The data for Flu-V33333-$His_6$ were very clear-cut (last line in Table 1): Addition of QSY7−S-tris-NTA caused no significant change in fluorescence, neither in the absence nor in the presence of $Ni^{2+}$. From this we conclude that the protein is rather extended, which prohibits FRET (Scheme 1B). This is in line with the known high flexibility of the modules with respect to each other seen in NMR spectroscopy.[18] However, when virus was added in molar excess over Flu-V33333-$His_6$ (taking into account that 12 V33333 molecules bind per virus particle)[3] then 80% of the fluorescein emission was quenched by QSY7−S-tris-NTA (last entry in Table 1). This finding nicely confirms ring formation of V33333 upon binding to the virus (Scheme 1D).

Similar results were obtained when Flu-MBP-V33333-$His_6$ was used in place of Flu-V33333-$His_6$ (next to last row in Table 1) except that they were less pronounced. Fluorescence emission was quenched by QSY7−S-tris-NTA and $Ni^{2+}$ to about 64% of the control already in the absence of virus, pointing to a less extended average conformation than observed with Flu-V33333-$His_6$. Nevertheless, in the presence of virus, quenching was further increased, reducing fluorescence emission to 32% of the control value. The moderate fluorescence change upon virus binding is not surprising because MBP is relatively large ($M_r \sim 44\,000$); thus, the statistically attached fluorescein labels cannot approach the C-terminal QSY7 label as closely as in Flu-V33333-$His_6$. Obviously, large tags like MBP are unfavorable for conformational analysis by FRET assays. Carrying out the same experiment with a receptor containing only three ligand-binding modules (Flu-MBP-V333-$His_6$), the addition of QSY7−S-tris-NTA led to quenching to 51%. This agrees well with the shorter distance between the fluorophore(s) attached to MBP and the quencher at the C-terminus. No further change in fluorescence was detected upon virus addition (Table 1). This also agrees well with the termini of the receptor molecule not coming close enough to each other for strong FRET when this truncated receptor construct is bound around the 5-fold axis of viral icosahedral symmetry.

## Discussion

The fluorescence data in Table 1 provide strong evidence that the VLDLR-mimicking protein V33333-$His_6$ forms a ring when bound to the surface of HRV2 particles (Scheme 1). For more detailed analysis of the binding geometry, HRV2 particles and V33333-$His_6$ were cocrystallized and analyzed by X-ray crystallography. The calculated structure showed that the V33333-$His_6$ molecules were indeed bound in a ring-like fashion around each of the 12 5-fold symmetry axes,[19] as suggested by the FRET data in Table 1.

Successful demonstration of ring formation by Flu-V33333-$His_6$ was made possible with the newly synthesized quencher−NTA conjugate, QSY7−S-tris-NTA, whereby QSY7 afforded strong quenching of the fluorescein label and tris-NTA provided for nanomolar affinity toward the $His_6$ tag of Flu-V33333-$His_6$. Consequently, the fluorescence assays could be performed at 10 nM fluorescein label and at 25−100 nM QSY7−S-tris-NTA, whereas micromolar concentrations of $His_6$-tagged protein and quencher−NTA had to be used in all previous FRET studies.[12−16]

The need for micromolar concentrations of quencher−tris-NTA conjugates in previous studies arose from the fact that the tris-NTA groups were always preloaded with exactly three $Ni^{2+}$ ions and subsequently mixed with $His_6$-tagged proteins in the absence of additional free $Ni^{2+}$ ions.[13−16] We actually tried this method in our first titration of Flu-$His_6$ with QSY7−S-tris-NTA and got almost the same titration curve (not shown) as seen with QSY7−NTA (Figure 1, open squares, apparent $K_d \sim 0.5\ \mu M$). In the presence of 2 $\mu$M $NiCl_2$, however, a much higher affinity of tris-NTA for $His_6$ was observed (Figures 1 and 2, open circles, apparent $K_d$ <10 nM). Systematic variation of the $Ni^{2+}$ concentration at 10 nM Flu-$His_6$ and 100 nM QSY7−S-tris-NTA (see Figure S8 in the Supporting Information) showed that 1−2 $\mu$M $Ni^{2+}$ is definitely required to saturate all three NTA functions in QSY7−S-tris-NTA (Figure S8) while 25−100 nM of QSY7−S-tris-NTA is clearly sufficient to saturate all $His_6$ tags when working at 2 $\mu$M $NiCl_2$ (Figure 2). Interestingly, 1−2 $\mu$M $Ni^{2+}$ was also sufficient to "activate" all NTA functions in the presence of 2 mM $Ca^{2+}$ (see lines 1 and 2 in Table 2), indicating very high selectivity of NTA functions for $Ni^{2+}$ over $Ca^{2+}$.

Another surprise was the finding that addition of EDTA (5 mM) to a preformed complex of Flu-$His_6$ and QSY7−S-tris-NTA-$(Ni^{2+})_3$ did not cause measurable dissociation within 1 h (Figure 2). The widely different $Ni^{2+}$ dependence before and after complex formation suggests that, in the absence of a $His_6$ tag, the individual NTA functions in QSY7−S-tris-NTA cannot retain bound $Ni^{2+}$ at <1 $\mu$M total $Ni^{2+}$ concentration, while after binding to $His_6$ the three $Ni^{2+}$ ions are trapped between $His_6$ peptide and tris-NTA for hours. According to this view, $Ni^{2+}$ could escape only after dissociation of the complete $His_6$ tag from the complex. In previous studies, the half-times for spontaneous dissociation of $His_6$ tags from different dye−tris-NTA conjugates were found to be in the range of ≥1 h.[13−15] In our model study with Flu-$His_6$ and QSY7−S-tris-NTA no measurable dissociation was seen within 1 h (Figure 2, closed squares), but this exceptional stability may be due to additional weak interactions between the two dye residues and should not be extrapolated to interaction of $His_6$ tags with tris-NTA functions in general. Fortunately, long-term stability is much less important than high affinity because quencher−NTA conjugates are intended for use in homogeneous FRET assays where all measurements are performed at equilibrium.

## Conclusion

QSY7−S-tris-NTA was prepared in good yield from the valuable precursors. It serves as a very succinct tool in FRET studies with $His_6$-tagged proteins where fluorescein (or ATTO-488, Oregon Green-488, etc.) are used as donors, as exemplified by the observation of ring formation of a flexible multimodular VLDL-receptor derivative attaching to the multivalent HRV2 capsid (Scheme 1). Another application of QSY7−S-tris-NTA would be the monitoring of specific binding between a $His_6$-tagged protein and any other molecule carrying a fluorescein-like label, as previously shown by Guignet et al. with QSY7−NTA.[12] In the latter study it was demonstrated that quencher−NTA conjugates are particularly useful in FRET assays because (i) the $His_6$-tagged protein need not be prelabeled and purified, (ii) in situ-labeling with quencher−NTA is site-specific for the $His_6$ tag, and (iii) excess of free quencher−NTA

(18) North, C. L.; Blacklow, S. C. *Biochemistry* **1999**, *38*, 3926–3935.
(19) Querol-Audi, J.; Konecsni, T.; Pous, J.; Carugo, O.; Fita, I.; Verdaguer, N.; Blaas, D. *FEBS Lett.* **2009**, *583*, 235–240.

in the solution does not influence donor emission. Now this method has been significantly improved by replacing QSY7−NTA with QSY7−S-tris-NTA, which has a 100-fold higher affinity for $His_6$ tags.

In the present study, we have shown that high affinity of tris-NTA for $His_6$ tags is only obtained at 1−2 $\mu$M free $Ni^{2+}$ concentration, while preformed 1:1 complexes of NTA functions and $Ni^{2+}$ appear to prematurely dissociate at submicromolar $Ni^{2+}$ concentrations, resulting in poor affinity for $His_6$ tags. These findings should also be relevant to heterogeneous assays in which $His_6$-tagged proteins are bound to mono-, bis-, or tris-NTA functions on solid surfaces or liposomes. It is anticipated that the full potential of all NTA-based methods can only be exploited if 1−2 $\mu$M free $Ni^{2+}$ is present during association of $His_6$ tags and NTA functions.

**Acknowledgment.** We thank Gerhard Spatz-Kümbel and Tanja Müller for technical assistance and Dr. Clemens Schwarzinger for ESI-MS data. This project was supported by the Austrian Science Foundation (FWF projects P17516, N00104, and P18384). A.R., K.S., J.P., and R.T. were supported by BMBF program "Nanobiotechnology".

**Supporting Information Available:** Experimental details on the synthesis of organic compounds, preparation of proteins and virus particles, labeling of $His_6$ peptide and proteins, general procedures, and fluorescence measurements of $Ni^{2+}$-independent effects by QSY7−S-tris-NTA and imidazole on Flu-$His_6$. This material is available free of charge via the Internet at http://pubs.acs.org.

JA807917T